Reaction Chemistry/Nanocrystal Property Relations in the Hot Injection Synthesis, the Role of the Solute Solubility

Sofie Abe,[†,‡] Richard K. Capek,[§,*] Bram De Geyter,[†,‡] and Zeger Hens[†,‡,*]

[†]Physics and Chemistry of Nanostructures and [‡]Center for Nano- and Biophotonics (NB-Photonics), Ghent University, B-9000 Ghent, Belgium, and [§]Schulich Faculty of Chemistry, Technion Haifa, 32000 Haifa, Israel

ABSTRACT Various literature studies show that increasing the concentration of free acid in the hot injection synthesis of colloidal nanocrystals raises the diameter of the resulting nanocrystals. We analyze this reaction chemistry/nanocrystal property relation by combining reaction simulations with an experimental study on a particular CdSe nanocrystal synthesis. We find that increasing the free acid concentration has the same effect on a real synthesis as raising the solute solubility in the simulations. Both lead to larger sizes and a deterioration of the size dispersion at constant reaction rate. Since free acids are used to coordinate the cation precursors in these syntheses, this leads to a meaningful link between a parameter in reaction simulations and the composition of an experimental reaction mixture. We thus explain the increase of the nanocrystal size with the acid concentration as resulting from an enhanced consumption of the solute by nanocrystal growth, which reduces the number of nanocrystals formed. This link between a simulation parameter and the composition of the reaction mixture provides a rational basis to further explore and understand reaction chemistry/nanocrystal property relations in the hot injection synthesis.

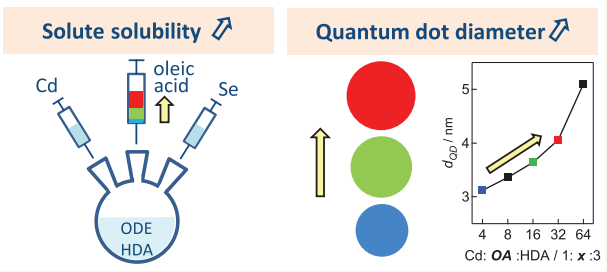

KEYWORDS: nanomaterials · colloids · quantum dots · reaction mechanism · kinetics

Over the last 15 years, colloidal semiconductor nanocrystals (NCs) or quantum dots (QDs) have proliferated as an alternate opto-electronic material used in photovoltaics,[1,2] photodetection,[3] color conversion, or fluorescent labeling. This application development requires materials with predefined sizes and low size dispersion in larger quantities. As a result, research on the hot injection synthesis—which is typically used to synthesize these materials—is focusing on optimization and scale-up. This involves the high-throughput screening, possibly combined with a rational design of experiments, of various synthesis parameters to achieve a desired end result.[4,5] What these studies essentially do is search for relations between the reaction conditions and the properties of the synthesized NCs, such as size and size dispersion. Importantly, by means of reaction simulations, this search for reaction chemistry/nanocrystal property relations can be linked to an improved understanding of the hot injection synthesis. For example, *via* high-throughput screening of a CdSe QD synthesis, it was found that the QD diameter d_{QD} (or radius r) at the end of the reaction can be increased by raising the precursor concentrations.[4] On the basis of synthesis modeling, this was later interpreted as an example of a more general tuning strategy, where the initial reaction rate is used to change the number of nuclei formed and, therefore, their final size at the end of the reaction.[6]

An alternative reaction chemistry/nanocrystal property relation used for nanocrystal size tuning in the hot injection synthesis that often appears in the literature, albeit not always used on purpose, is that between the concentration of the free acid and the nanocrystal size. For various materials, including II–VI,[5,7–10] III–V,[11,12] and IV–VI[13,14] semiconductors, various metal oxides,[15] and

* Address correspondence to capek@technunix.technion.ac.il, zeger.hens@ugent.be.

Received for review June 4, 2012 and accepted January 15, 2013.

Published online January 15, 2013
10.1021/nn3059168

metals,[16] it is observed that d_{QD} increases with the carboxylic acid concentration. This relation is interpreted as either reflecting a suppression of the nucleation related to an increase of the solubility of the reagents with increasing free acid concentration[9,16] or resulting from an enhanced reactivity during the nucleation stage at lower free acid concentrations.[7,11,13,14] Opposite from these conjectures, Owen *et al.* showed in a quantitative study on CdSe QDs synthesized using phosphonic acids that a reduction of the phosphonic acid concentration systematically leads to the formation of more QDs, while the overall reaction rate remains unchanged.[17]

Here, we use a combination of reaction simulations and experimental synthesis screening to understand the role of free acids in the hot injection synthesis. As a starting point, we consider that cation precursors are usually brought in solution as coordinated complexes, where in particular carboxylic (CA) or phosphonic acids are often used to form metal carboxylate or metal phosphonate complexes. With CdSe QDs stabilized by carboxylate ligands, a pronounced exchange of surface-bound carboxylates with free acids has been reported, indicating an additional coordination of the QDs by excess acids.[18] Therefore, free acids may also stabilize the actual solute or monomer, thereby enhancing its solubility. In line with this assumption, we use reaction simulations to show that increasing the monomer solubility at constant reaction rate results in larger nanocrystals since monomer consumption by growth is enhanced relative to consumption by nucleation. Next, this size tuning concept is experimentally studied by means of a CdSe synthesis that has been used before to demonstrate high-throughput[4] and design-of-experiment synthesis[5] optimization and to analyze the link between d_{QD} and the initial reaction rate.[6] For this reaction, we find that the reaction rate is independent of the CA concentration while d_{QD} and the size dispersion (σ_d) increase with the CA concentration. Exploring the parameter space of the reaction simulations, we find that the monomer solubility is the only simulation parameter where an increase in nanocrystal diameter at constant reaction rate concurs with a deterioration of the size dispersion, as observed experimentally. Hence, we conclude that free CA affects the outcome of a real hot injection synthesis in the same way as the monomer solubility does in the simulations. This does not change the reaction rate, yet it affects the time where monomer consumption by nucleation is overtaken by growth. The kinetics of nucleation and growth of isotropic QDs are thus dominated not only by the formation rate of the monomer[6] but also by its stabilization in the reaction mixture. Furthermore, combining literature data with additional experiments, we argue that these results can be extended to syntheses using phosphonic and phosphinic acids, and we use the simulation results to rationalize the dependence between size and acid concentration in binary ligand systems.

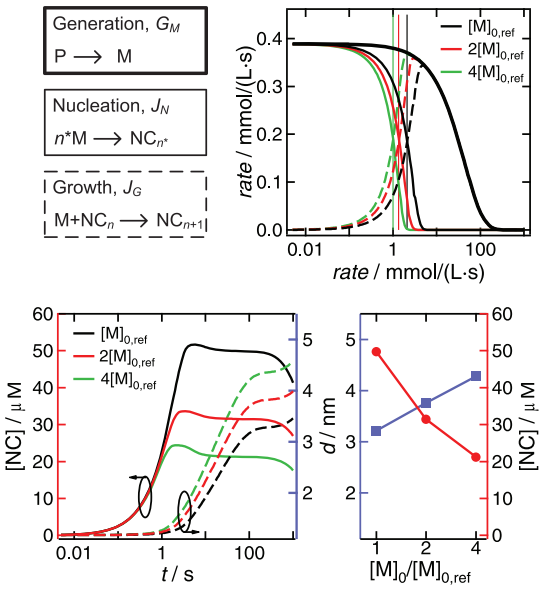

Figure 1. (a) Processes considered in the reaction simulations. Monomers M are generated from precursors at a rate G_M and consumed by nucleation (rate J_N) of new and growth (rate J_G) of existing NCs. (b) Variation of (bold line) G_M, J_N (solid line), and J_G (dashed line) with time for different values of the monomer solubility as indicated. The vertical lines indicate the time where the monomer consumption rate by nucleation and growth is equal. (c) Time development (solid lines, red axis) of nanocrystal concentration [NC] and (dashed lines, blue axis) nanocrystal diameter d_{QD} for the respective simulations shown in panel b. (d) [NC] (red) and d_{QD} (blue) at 98% yield as a function of the monomer solubility.

RESULTS

Reaction Simulations. The reaction simulations are carried out using the approach published before by Kwon *et al.*[19] and Abe *et al.*[6] and outlined in more detail in the Supporting Information (S1.1). As depicted in Figure 1a, this involves a kinetic scheme in which the injected precursors P first react to form a monomer M.[20,21] For simplicity, we take the rate G_M of monomer generation as first-order in the precursor concentration. Next, the generated monomers are consumed by nucleation and growth. As shown in Figure 1a, nucleation is modeled as a process in which new NCs are formed out of a critical number n^* of monomers, with a nucleation rate J_N according to classical nucleation theory. Growth is described as the incorporation of monomers in existing NCs, where the overall consumption of monomers by growth J_G is expressed using the growth rate per NC $j_G = dr/dt$ as proposed by Talapin *et al.*[22] (D, monomer diffusion coefficient; v_0, monomer volume; γ, surface tension of the NC; V_m, molar volume of the QD material; R, gas constant; S, monomer supersaturation; N_A, Avogadro's number; T, absolute temperature; $[M]_0$, monomer solubility; k_g^∞, monomer adsorption

rate constant on a flat surface; and α, transfer coefficient of the crystal growth reaction):

$$J_N = \frac{2D}{v_0^{5/3}} \exp\left(-\frac{16\pi\gamma^3 V_m^2 N_A}{3(RT)^3(\ln S)^2}\right) \quad (1)$$

$$j_G = DV_m[M]_0 \left[\frac{S - \exp\left(-\frac{2\gamma V_m}{rRT}\right)}{r + \frac{D}{k_g^\infty}\exp\left(\alpha\frac{2\gamma V_m}{rRT}\right)}\right] \quad (2)$$

The black lines in Figure 1b,c represent the variation of G_M, J_N, and J_G and the concomitant change of the amount of nanocrystals n_{NC} and d_{QD} for a synthesis simulation using the reference parameters as given in the Supporting Information (S1.2). Figure 1b shows that, at the start of the reaction, the generated monomers are almost exclusively consumed by nucleation. As n_{NC} grows, monomer consumption by growth becomes more important and eventually completely suppresses the nucleation. A characteristic time for the takeover of nucleation by growth is the moment where $J_N = J_G$, which is indicated by the vertical lines in Figure 1b. Clearly, expediting this takeover while keeping the reaction rate G_M constant will reduce n_{NC} and thus increase the final NC diameter. Looking at eq 1 and eq 2, one sees that J_N depends on the monomer supersaturation S, while j_G scales with the monomer solubility $[M]_0$. This indicates that, even when the reaction rate is kept constant, a change of $[M]_0$ will influence the balance between nucleation and growth, where a larger solubility leads to an earlier takeover. The red and green curves in Figure 1b show G_M, J_N, and J_G for reaction simulations where $[M]_0$ is raised to 2 and 4 times the reference value, while keeping all other parameters fixed. In line with the above reasoning, one sees that the larger $[M]_0$, the sooner J_G exceeds J_N. As indicated in Figure 1c, this reduces n_{NC}, resulting in larger NCs at the end of the reaction. Hence, we conclude that a change of $[M]_0$ allows for size tuning at constant reaction rate in the hot injection synthesis since it influences the takeover of nucleation by growth.

Experimental Results. To relate the model predictions on size tuning by $[M]_0$ to the influence of the free acid concentration on nanocrystal size in an experimental hot injection synthesis, we studied the relation between the concentration of free carboxylic acid, the reaction rate, and the QD diameter in a typical zinc blende CdSe QD synthesis. This involves the injection of trioctylphosphine selenide (TOP-Se) in a hot mixture of cadmium oleate ($Cd(OA)_2$), oleic acid (OA), and hexadecylamine (HDA) in octadecene (ODE).[4−6] Different reactions are characterized by the ratio $Cd(OA)_2$/total OA/HDA, where total OA refers to the sum of the OA used to coordinate the Cd^{2+} and excess free OA. For the different reactions, only total OA is changed by changing the amount of free OA. The reactions are analyzed by absorption spectroscopy, using either purified aliquots taken at different times after the injection or only at the end of the reaction, which yields the diameter d_{QD}, the size dispersion σ_d, and the amount of CdSe n_{CdSe}.[23]

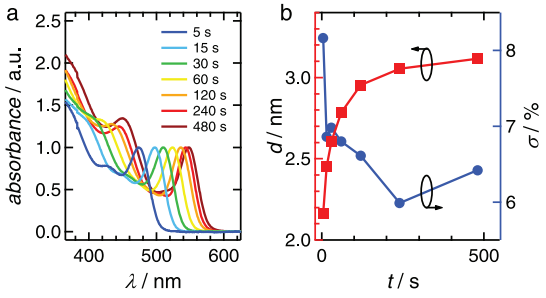

Figure 2. (a) Absorption spectra of aliquots taken at the indicated times after injection for a CdSe synthesis using $Cd(OA)_2$ and TOP-Se as precursors in ODE. Cd/OA/HDA = 1:4:3. (b) Evolution of d_{QD} (red) and σ_d (blue) with time as calculated from the spectra shown in panel a.

Figure 2a gives an example of absorption spectra recorded on aliquots for a 1:4:3 (Cd/OA/HDA) synthesis. In line with previously published data on this synthesis, the absorption peak of the first exciton ($\lambda_{1S_e-1S_h}$) progressively shifts to longer wavelengths and tends toward a limiting value at 480 s. Obviously, d_{QD} follows the same trend (Figure 2b). The size dispersion on the other hand reaches a minimum value at around 240 s—indicative of size focusing—and slightly increases afterward.

Figure 3a shows the absorption spectra of aliquots taken after 480 s of reaction time for syntheses where the Cd/OA/HDA ratio is progressively raised from 1:4:3 to 1:64:3. The red shift and broadening of the first exciton absorption peak already indicate that this results in a concomitant increase of both d_{QD} and σ_d, which change from about 3.1 to 5.1 nm and 6.3 to 16.9%, respectively (Figure 3b). For three different Cd/OA/HDA ratios, we have determined the time development of n_{CdSe}, d_{QD}, and the number of QDs n_{QD} by taking aliquots and analyzing the respective absorption spectra (see Supporting Information S2.2−S2.4).[6] As indicated in Figure 3c, the time development of n_{CdSe}, which directly reflects the reaction rate, is almost independent of the amount of OA. A global fit of the three curves assuming G_M to be first-order in TOP-Se and $Cd(OA)_2$ yields a second-order rate constant of 0.11 L/(mol·s), a number in line with previously published values.[6] On the other hand, raising [OA] significantly reduces the amount of QDs formed (see Figure 3d). As the final yield remains constant, this obviously leads to an increase of d_{QD}.

DISCUSSION

The increase of d_{QD}—and decrease of n_{QD}—with increasing carboxylic acid concentration as shown here for a particular CdSe QD synthesis has been

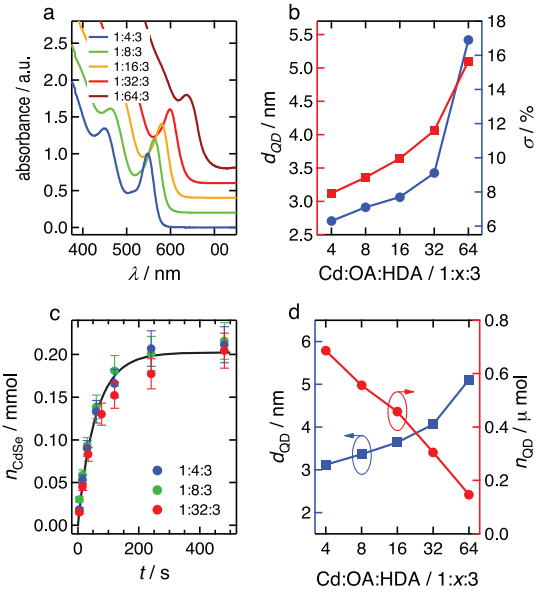

Figure 3. (a) Absorption spectra of aliquots taken after 480 s of reaction time for different Cd/OA/HDA ratios. (b) Values of d_{QD} (red) and σ_d (blue) after 480 s reaction time for the different reactions shown in panel a. (c) Amount of CdSe formed as a function of time for three different Cd/OA/HDA ratios as indicated. The solid line is a best global fit assuming G_M to be first-order in $Cd(OA)_2$ and TOP-Se. (d) Values of d_{QD} and n_{QD} as determined by stopping reactions with different Cd/OA/HDA ratios as indicated after 480 s. All data are obtained using the standard amounts and temperatures as indicated in the Methods section.

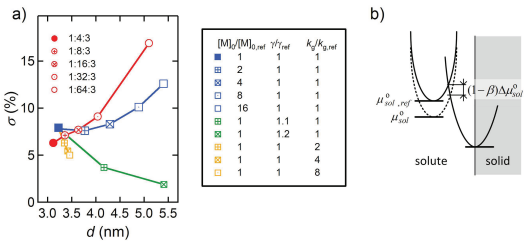

Figure 4. (a) Size dispersion as a function of diameter for reaction simulations as a function of $[M]_0$ (blue), γ (green), and k_g (orange) (data taken after 128 s) and experimental synthesis (red) for the indicated Cd/OA/HDA combinations (data taken after 480 s). The table lists the particular parameter values used in each simulation. (b) Scheme showing how a stabilization of the monomer—linked to a reduction of its standard chemical potential—increases the activation energy for monomer adsorption and thus lowers k_g.

reported for a wide range of colloidal nanocrystals, including semiconductors, metal oxides, and metals.[5,7−16] Various authors consider this relation as counterintuitive. Since free acids are supposed to act as ligands, raising their concentration should increase the ligand density on the QD surface and thus hamper nanocrystal growth.[14] It is therefore proposed that the increase of the number of nanocrystals formed when lowering the free acid concentration reflects an enhanced reactivity during the nucleation stage. An alternate interpretation of the relation starts from the idea that the supersaturation reflects the ratio between the actual concentration of the metal precursor and its solubility. It is then assumed that a stabilizing agent such as a carboxylic acid increases the solubility of the metal precursor and thus suppresses the nucleation by reducing the supersaturation.[9,16,24] Opposite from both interpretations, we find that the free acid concentration does not affect the overall reaction rate, which indicates that the observed size tuning does not result from an enhanced reactivity at low carboxylic acid concentration or a suppressed nucleation at high carboxylic acid concentration. A similar finding has been reported by Owen *et al.*, who showed that the reaction rate in a CdSe synthesis using dimethylcadmium and TOP-Se as the precursors in a mixture of octadecylphosphonic acid (ODPA) and trioctylphospine oxide as the coordinating solvent does not depend on the phosphonic acid concentration, while larger QDs are obtained if the ODPA concentration is raised.

The simulations are based on the idea that the formation of a monomer out of the precursors precedes the nucleation and growth of nanocrystals, where the supersaturation is defined as the ratio between the actual monomer concentration and its solubility. Both for the simulations and for the experimental CdSe reaction used here, the rate of the monomer formation determines the rate of CdSe formation by nucleation and growth.[6] According to the simulations, size tuning is possible under the conditions of a constant reaction rate—as observed experimentally—by accelerating or delaying the takeover of nucleation by growth, where an earlier takeover leads to less and thus larger nanocrystals. This is achieved by varying the monomer solubility $[M]_0$. However, size tuning at constant reaction rate can also result from an increase of the free energy barrier for nucleation, which implies that nucleation requires a higher supersaturation, or from an increase of the monomer adsorption rate k_g^∞ since both conditions favor growth. In principle, $[M]_0$ corresponds to the amount of unreacted monomer at the end of the reaction. However, regardless of the oleic acid concentration, the CdSe synthesis we use has a yield of about 100%. This indicates that $[M]_0$ is considerably smaller than the initial concentration of $Cd(OA)_2$, which unfortunately prevents a reliable determination of $[M]_0$ by directly measuring it, and thus confirms the link between the carboxylic acid concentration and the monomer solubility.

To analyze the alternative interpretations, the Supporting Information shows simulation results where we change either the free energy barrier for nucleation, by varying the QD surface tension γ (S1.3), or the monomer adsorption rate constant k_g^∞ (S1.4). The key result is summarized in Figure 4a. We find that an increase of both γ and k_g^∞ leads to larger nanocrystals. However, the increase of d_{QD} comes with a marked reduction of the size dispersion σ_d. This effect can be

understood by considering that the enhanced consumption of monomers by growth is achieved either by raising the supersaturation (due to an increase of γ) or k_g^∞. Both conditions enhance the size focusing, which leads to a reduction of σ_d for larger diameters. Opposite from this, increasing the free acid concentration in the CdSe synthesis studied deteriorates the size dispersion (see Figure 3b and Figure 4a), a result also reported in the literature for other material systems.[7]

The observed deterioration of the size dispersion with increasing carboxylic acid concentration can be understood by linking it to an enhanced monomer solubility. In general, the solubility $[M]_0$ is related to the standard free energy of dissolution, which is defined as the difference $\mu^\circ_{sol} - \mu^\circ_s$ between the standard chemical potential of the solute and the solid (c°, standard concentration):

$$\frac{[M]_0}{c^\circ} = \exp\left(-\frac{\mu^\circ_{sol} - \mu^\circ_s}{RT}\right) \quad (3)$$

An increase in solubility thus implies a lowering of μ°_{sol}. At the same time, the solubility is equal to the ratio of the monomer desorption k_d^∞ and adsorption k_g^∞ rate constants at a flat substrate.

$$[M]_0 = \frac{k_d^\infty}{k_g^\infty} \quad (4)$$

Hence, if $[M]_0$ changes, either k_d^∞, k_g^∞, or both must change as well. As indicated by Figure 4b, one can expect that a lowering of μ°_{sol} will increase the activation energy for growth and thus reduce k_g^∞. This shifts the reaction from diffusion control ($D/k_g^\infty \ll 1$) toward kinetic control ($D/k_g^\infty \gg 1$), that is, out of the size-focusing regime.[22] As shown in the Supporting Information, this enhances the defocusing of the size distribution during nucleation, which is not compensated by more focusing during growth. As confirmed by the simulation results shown in Figure 4a (blue markers), this leads to an increase of d_{QD} with a concomitant deterioration of the size dispersion, in agreement with the experimental results. Additional simulations shown in the Supporting Information (S1.5) indicate that the decrease of k_g^∞ with increasing $[M]_0$ is essential to retrieve a deteriorated size dispersion for larger diameters. For the simulation results shown in Figure 4, we have kept k_d^∞ fixed such that k_g^∞ scales with the inverse of $[M]_0$. A further deterioration of the size dispersion would occur if, as suggested in the literature, free acids would facilitate nanocrystal dissolution and thus raise k_d^∞.[17,25] In summary, we conclude that free acids raise d_{QD} most likely since they increase the monomer solubility. This promotes monomer consumption by growth over consumption by nucleation. As a result, less nanocrystals are formed, which thus grow to larger sizes while the reaction rate remains fixed. For reactions such as the InP synthesis where growth is accomplished by a ripening mechanism, free acids are supposed to promote the dissolution of monomers or small clusters from existing nanocrystals.[12,24] While this involves a different mechanism of size control *via* the free acid concentration, this is in line with the interpretation following from our work that free acids stabilize solutes and thus enhance their solubility.

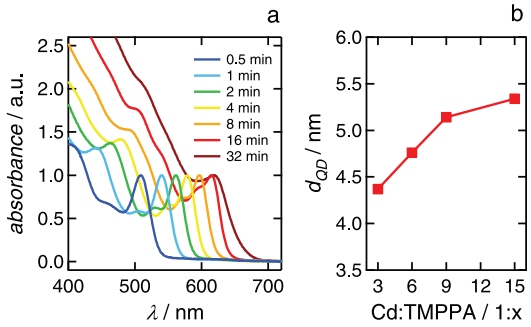

Figure 5. (a) Absorption spectrum of aliquots taken at the indicated times after injection for a CdSe synthesis using a Cd/TMPPA complex and TOP-Se as precursors in ODE. Cd/TMPPA = 1:9. (b) Diameters obtained when stopping the reaction after 16 min as a function of the Cd/TMPPA ratio.

Although the link between carboxylic acid concentration and nanocrystal size has been well-documented in the literature, the question arises as to how general it is. As mentioned before, similar results of size tuning at constant reaction rate have been reported for CdSe synthesized using octadecylphosphonic acid. On the other hand, it has been shown that the addition of trimethylpentylphosphinic acid (TMPPA) to an OA-based CdSe synthesis to form a binary ligand system decreases d_{QD} up to TMPPA/OA ratios of ≈1:2. At larger concentrations of TMPPA, d_{QD} increases with increasing TMPPA concentration.[9] The reduction of d_{QD} was interpreted in terms of the stronger binding of TMPPA to CdSe nanocrystals. This reduces the nanocrystal surface tension, which is supposed to promote nucleation. As shown in Figure 4, our simulations show a similar result. Reading the figure by going from γ/γ_{ref} = 1.2 to γ/γ_{ref} = 1, a reduction of the surface tension indeed leads to smaller particles when the reaction rate is kept constant. This happens since a reduction of the surface tension makes stable nuclei form at a lower supersaturation. As a result, growth is delayed (see eq 2) so that more particles nucleate with a smaller size in the end.

Changing the nanocrystal surface tension is an effect TMPPA additions can have in a binary ligand system. This, however, is different from its intrinsic effect on the monomer solubility. Figure 5a shows absorption spectra of aliquots taken during a CdSe synthesis containing TMPPA as the only complexing agent. In this case, the nanocrystals grow up to 16 min after injection, after which a ripening regime sets in similar to the OA-based synthesis.[6] Also for this reaction, we find that an increase of the TMPPA concentration leads to larger

nanocrystals (Figure 5b). Although the CdSe synthesis using TMPPA is less ideal for this study—the reaction rate also changes with TMPPA concentration (see Supporting Information)—this result is in line with what we obtained using carboxylic acids. This indicates that the effect of TMPPA additions to a CdSe synthesis using carboxylic acids as the complexing agent can be understood as the result of two opposing effects. On the one hand, the stronger binding of the TMPPA to the nanocrystals lowers their surface tension; on the other hand, both TMPPA and OA enhance the monomer solubility. At low TMPPA concentrations, the first effect dominates and d_{QD} decreases with increasing additions of TMPPA. At higher concentration, the surface tension reduction stops, for example, since the nanocrystal ligand shell is composed solely of TMPPA, and the solubility enhancement leads to an increase of d_{QD}, as is observed in a synthesis using TMPPA or OA only.

CONCLUSION

In summary, we have analyzed the often observed increase of the final nanocrystal size and size dispersion with the free acid concentration—an example of what we call a reaction chemistry/nanocrystal property relation—in the hot injection synthesis by bringing together reaction simulations and an experimental study on a particular CdSe QD synthesis. We find that the effect of the free acid concentration on the size and the size dispersion of the nanocrystals in the experimental synthesis agrees with the influence of the monomer solubility on the nanocrystal properties in the simulations. An enhanced monomer solubility promotes the monomer consumption by growth, which shortens the nucleation and thus reduces the number of nanocrystals formed. This result indicates that, in this case, the kinetics of nucleation and growth of isotropic QDs are determined by the properties of the solute, such as its formation rate[6] and, as shown here, its stabilization by ligands. Moreover, our work demonstrates that it is possible to link directly the composition of the reaction mixture to simulation parameters, thereby providing a key to a more efficient, modeling-based study of reaction chemistry/nanocrystal property relations in the hot injection synthesis. With respect to size tuning, we conclude that changing the free acid concentration is not the best tuning strategy since a higher free acid concentration reduces size focusing and thus deteriorates the size dispersion.

METHODS

CdSe Quantum Dot Synthesis (Oleic Acid as Complexing Agent). CdSe QDs were synthesized following a previously described procedure.[6] In brief, a mixture of cadmium oleate (0.2 mmol), HDA (0.6 mmol), oleic acid (variable amount, molar ratio Cd/OA/HDA 1:*x*:3 as indicated), and ODE (total volume = 10 mL) was stirred under a nitrogen flow for 30 min at room temperature and 60 min at 100 °C. The nitrogen flow was stopped, and still under nitrogen, the temperature was raised to 245 °C and 2 mL of a 1 M TOP-Se solution (2 mmol) were injected, and the reaction was performed at 230 °C. Aliquots were taken after specific reaction times, weighed, dissolved in a 1:5 mixture of OA and toluene, and precipitated and resuspended twice using methanol and toluene as the nonsolvent and the solvent, respectively. For the synthesis work, toluene (>99.8%), methanol (>99.85%), and 2-propanol (>99.7%) were purchased from Fiers; oleic acid (90%) and cadmium oxide (CdO, >99.99% metal bases) were purchased from Sigma-Aldrich; selenium (99.999%) and 1-octadecene (ODE, tech.) were purchased from Alfa Aesar; hexadecylamine (HDA, 90%) was purchased from Merck, and trioctylphosphine (TOP, 97%) was purchased from Strem.

CdSe Quantum Dot Synthesis (TMPPA as Complexing Agent). A cadmium precursor was prepared by mixing CdO and TMPPA in a 1:3 molar ratio, flushing with a nitrogen flow at 100 °C for 1 h, and dissolving the cadmium oxide under a nitrogen atmosphere at 300 °C until the mixture became clear. CdSe QDs were synthesized similar to the procedure described above using oleic acid as complexing agent. A mixture of the cadmium precursor and TMPPA (variable amount, molar ratio 1:*x* as indicated) was filled up to a total volume of 9 mL at room temperature. The reaction mixture was stirred under a nitrogen flow for 30 min at room temperature and 60 min at 100 °C. Still under nitrogen, the temperature was raised to the injection temperature (300 °C), 1 mL of a solution of a 1 M TOP-Se solution was injected, and the reaction was performed at a growth temperature of 290 °C. Aliquots of the final reaction products were weighed, dissolved in chloroform, and precipitated using a 1:1 mixture of methanol and acetonitrile. After resuspension in chloroforme, they were precipitated again using an excess of methanol.

Aliquot Analysis by UV–Vis Spectroscopy. UV–vis spectra of purified, weighted aliquots were recorded for quantitative analysis with a Perkin-Elmer Lambda 2 spectrophotometer.[6] Using the zb-CdSe sizing curve,[23] the mean QD diameter, d_{QD}, is calculated from the peak wavelength of the first exciton transition using the sizing curve of either zb-CdSe (syntheses with OA as complexing agent)[23] or wz-CdSe (syntheses with TMPPA as complexing agent),[26] while the size distribution is estimated from the half-width at half-maximum (hwhm_λ) of the same absorption peak:

$$\sigma_d = \frac{1}{d_{QD}} \frac{\mathrm{hwhm}_\lambda}{\sqrt{2\ln 2}} \left| \frac{\mathrm{d}(d_{QD})}{\mathrm{d}\lambda} \right|$$

Here, the derivative $\mathrm{d}(d_{QD})/\mathrm{d}\lambda$ is calculated using the zinc blende CdSe sizing curve. The amount of CdSe formed n_{CdSe} is obtained from the average absorbance of a diluted aliquot at 300, 320, and 340 nm, which is directly proportional to the volume fraction of CdSe.[23]

Reaction Simulations. Modeling of the QD synthesis was done by implementing the equations given in the Supporting Information into COMSOL Multiphysics, a commercially available finite-element partial differential equation solver. The parameters used for the reference simulation are given in the Supporting Information.

Conflict of Interest: The authors declare no competing financial interest.

Acknowledgment. Z.H. acknowledges the FWO-Vlaanderen (G.0760.12, G.0794.10), BelSPo (IAP 7.35, photonics@be), and EU-FP7 (ITN Herodot, Grant Agreement No. 214954) for funding. S.A. acknowledges the IWT-Vlaanderen (Agency for Innovation by Science and Technology in Flanders) for a scholarship.

Supporting Information Available: Details on the reaction simulations (model equations, reference parameter values, influence of surface tension and growth rate on size and size

dispersion), and the experimental CdSe synthesis using either oleic acid or TMPPA. This material is available free of charge *via* the Internet at http://pubs.acs.org.

REFERENCES AND NOTES

1. Tang, J.; Kemp, K. W.; Hoogland, S.; Jeong, K. S.; Liu, H.; Levina, L.; Furukawa, M.; Wang, X.; Debnath, R.; Cha, D.; *et al.* Colloidal-Quantum-Dot Photovoltaics Using Atomic-Ligand Passivation. *Nat. Mater.* **2011**, *10*, 765–771.
2. Luther, J. M.; Law, M.; Beard, M. C.; Song, Q.; Reese, M. O.; Ellingson, R. J.; Nozik, A. J. Schottky Solar Cells Based on Colloidal Nanocrystal Films. *Nano Lett.* **2008**, *8*, 3488–3492.
3. Rauch, T.; Boeberl, M.; Tedde, S. F.; Fuerst, J.; Kovalenko, M. V.; Hesser, G.; Lemmer, U.; Heiss, W.; Hayden, O. Near-Infrared Imaging with Quantum-Dot-Sensitized Organic Photodiodes. *Nat. Photonics* **2009**, *3*, 332–336.
4. Chan, E. M.; Xu, C.; Mao, A. W.; Han, G.; Owen, J. S.; Cohen, B. E.; Milliron, D. J. Reproducible, High-Throughput Synthesis of Colloidal Nanocrystals for Optimization in Multidimensional Parameter Space. *Nano Lett.* **2010**, *10*, 1874–1885.
5. Protiere, M.; Nerambourg, N.; Renard, O.; Reiss, P. Rational Design of the Gram-Scale Synthesis of Nearly Monodisperse Semiconductor Nanocrystals. *Nanoscale Res. Lett.* **2011**, *6*, 472.
6. Abe, S.; Capek, R. K.; De Geyter, B.; Hens, Z. Tuning the Postfocused Size of Colloidal Nanocrystals by the Reaction Rate: From Theory to Application. *ACS Nano* **2012**, *6*, 42–53.
7. Yu, W.; Peng, X. Formation of High-Quality CdS and Other II−VI Semiconductor Nanocrystals in Noncoordinating Solvents: Tunable Reactivity of Monomers. *Angew. Chem., Int. Ed.* **2002**, *41*, 2368–2371.
8. Bullen, C.; Mulvaney, P. Nucleation and Growth Kinetics of CdSe Nanocrystals in Octadecene. *Nano Lett.* **2004**, *4*, 2303–2307.
9. van Embden, J.; Mulvaney, P. Nucleation and Growth of CdSe Nanocrystals in a Binary Ligand System. *Langmuir* **2005**, *21*, 10226–10233.
10. Dai, Q.; Kan, S.; Li, D.; Jiang, S.; Chen, H.; Zhang, M.; Gao, S.; Nie, Y.; Lu, H.; Qu, Q.; *et al.* Effect of Ligands and Growth Temperature on the Growth Kinetics and Crystal Size of Colloidal CdSe Nanocrystals. *Mater. Lett.* **2006**, *60*, 2925–2928.
11. Battaglia, D.; Peng, X. Formation of High Quality InP and InAs Nanocrystals in a Noncoordinating Solvent. *Nano Lett.* **2002**, *2*, 1027–1030.
12. Baek, J.; Allen, P. M.; Bawendi, M. G.; Jensen, K. F. Investigation of Indium Phosphide Nanocrystal Synthesis Using a High-Temperature and High-Pressure Continuous Flow Microreactor. *Angew. Chem., Int. Ed.* **2011**, *50*, 627–630.
13. Hines, M.; Scholes, G. Colloidal PbS Nanocrystals with Size-Tunable Near-Infrared Emission: Observation of Post-Synthesis Self-Narrowing of the Particle Size Distribution. *Adv. Mater.* **2003**, *15*, 1844–1849.
14. Dai, Q.; Zhang, Y.; Wang, Y.; Wang, Y.; Zou, B.; Yu, W. W.; Hu, M. Z. Ligand Effects on Synthesis and Post-Synthetic Stability of PbSe Nanocrystals. *J. Phys. Chem. C* **2010**, *114*, 16160–16167.
15. Jana, N.; Chen, Y.; Peng, X. Size- and Shape-Controlled Magnetic (Cr, Mn, Fe, Co, Ni) Oxide Nanocrystals *via* a Simple and General Approach. *Chem. Mater.* **2004**, *16*, 3931–3935.
16. Shevchenko, E. V.; Talapin, D. V.; Schnablegger, H.; Kornowski, A.; Festin, R.; Svedlindh, P.; Haase, M.; Weller, H. Study of Nucleation and Growth in the Organometallic Synthesis of Magnetic Alloy Nanocrystals: The Role of Nucleation Rate in Size Control of $CoPt_3$ Nanocrystals. *J. Am. Chem. Soc.* **2003**, *125*, 9090–9101.
17. Owen, J. S.; Chan, E. M.; Liu, H.; Alivisatos, A. P. Precursor Conversion Kinetics and the Nucleation of Cadmium Selenide Nanocrystals. *J. Am. Chem. Soc.* **2010**, *132*, 18206–18213.
18. Fritzinger, B.; Capek, R. K.; Lambert, K.; Martins, J. C.; Hens, Z. Utilizing Self-Exchange To Address the Binding of Carboxylic Acid Ligands to CdSe Quantum Dots. *J. Am. Chem. Soc.* **2010**, *132*, 10195–10201.
19. Kwon, S. G.; Piao, Y.; Park, J.; Angappane, S.; Jo, Y.; Hwang, N.-M.; Park, J.-G.; Hyeon, T. Kinetics of Monodisperse Iron Oxide Nanocrystal Formation by "Heating-Up" Process. *J. Am. Chem. Soc.* **2007**, *129*, 12571–12584.
20. Steckel, J. S.; Yen, B. K. H.; Oertel, D. C.; Bawendi, M. G. On the Mechanism of Lead Chalcogenide Nanocrystal Formation. *J. Am. Chem. Soc.* **2006**, *128*, 13032–13033.
21. Liu, H.; Owen, J. S.; Alivisatos, A. P. Mechanistic Study of Precursor Evolution in Colloidal Group II−VI Semiconductor Nanocrystal Synthesis. *J. Am. Chem. Soc.* **2007**, *129*, 305–312.
22. Talapin, D.; Rogach, A.; Haase, M.; Weller, H. Evolution of an Ensemble of Nanoparticles in a Colloidal Solution: Theoretical Study. *J. Phys. Chem. B* **2001**, *105*, 12278–12285.
23. Capek, R. K.; Moreels, I.; Lambert, K.; De Muynck, D.; Zhao, Q.; Vantomme, A.; Vanhaecke, F.; Hens, Z. Optical Properties of Zincblende Cadmium Selenide Quantum Dots. *J. Phys. Chem. C* **2010**, *114*, 6371–6376.
24. Allen, P. M.; Walker, B. J.; Bawendi, M. G. Mechanistic Insights into the Formation of InP Quantum Dots. *Angew. Chem., Int. Ed.* **2010**, *49*, 760–762.
25. Yordanov, G. G.; Yoshimura, H.; Dushkin, C. D. Fine Control of the Growth and Optical Properties of CdSe Quantum Dots by Varying the Amount of Stearic Acid in a Liquid Paraffin Matrix. *Colloids Surf., A* **2008**, *322*, 177–182.
26. Jasieniak, J.; Smith, L.; van Embden, J.; Mulvaney, P.; Califano, M. Re-examination of the Size-Dependent Absorption Properties of CdSe Quantum Dots. *J. Phys. Chem. C* **2009**, *113*, 19468–19474.